Physical Waveform Optimization for Multiple-Beam Multifunction Digital Arrays

(Invited Paper)

Patrick M. McCormick and Cenk Sahin
Air Force Research Lab
Sensors Directorate
Wright-Patterson AFB, OH, USA

Shannon D. Blunt
University of Kansas
Radar Systems Lab (RSL)
Lawrence, Kansas, USA

Justin G. Metcalf
University of Oklahoma
Advanced Radar Research Center
Norman, Oklahoma, USA

***Abstract*—The co-design of multiple RF functions provides the means to efficiently use the resources available for transmission (i.e. time, frequency, space, and power). Digital array technology supports simultaneous control over all domains of diversity through independent generation of the waveform emitted by each antenna element. The Far-field Radiated Emission Design (FFRED) formulation considers the efficient use of all available resources by simultaneously performing multiple functions in the same frequency band via spatially separated beams. The waveforms in the FFRED problem are constrained to have attractive signal properties via reduction in peak-to-average power ratio (PAPR) to increase power efficiency. This design constraint is shown to leverage the spatial orthogonal complement to the desired transmission directions so as to not interfere with the RF functions. Here, the FFRED problem is formulated as a gradient-based optimization with reduced computational complexity relative to the previous alternating projection implementation. For a certain initialization, the optimized waveforms are shown to be near-optimal in terms of minimal energy within the orthogonal complement.**

I. Introduction

Solutions to the problem of spectral congestion can be split into two categories: 1) cohabitation between RF users within the same band where no cooperation is assumed (e.g. dynamic spectrum access); and 2) co-design of multiple RF functions within the same band, where there is full control over the interplay between the functions (e.g. time-division multiple access, beam-scheduling in radar). Here, the co-design problem is considered from the perspective of utilizing spatial degrees-of-freedom to limit the mutual interference between different functions as a means to make efficient use of both time and frequency resources. The fully digital array facilitates this concept by providing the capability to perform multiple simultaneous functions from the same aperture by supporting independent control of the waveforms emitted by each antenna element [1]–[5]. Thus by utilizing this technology, the spatially-separated multifunction capability can be viewed as a waveform design problem that places each desired RF function within a separate beam on transmit.

In [6]–[8], it was shown that a set of physically realizable frequency-modulated (FM) waveforms can be optimized using the Error Reduction Algorithm [9] to emit simultaneous, pulsed radar and communications signals in different spatial directions, a formulation denoted as Far-Field Radiated Emission Design (FFRED). The FFRED approach considers the transmission of multiple simultaneous signals (e.g. radar and/or communications signals) from a digital array while considering practical waveform attributes (e.g. constant amplitude, power efficiency). It was shown that by utilizing the spatial orthogonal complement to the desired transmission directions, the optimized waveforms can be constrained to be constant amplitude. Here, the FFRED objective function is reexamined for gradient-based optimization to reduce computational complexity and to minimize the energy within the orthogonal complement required to obtain a viable solution.

A relaxed form of the FFRED objective function from [7] is defined that reduces the computational cost of finding a set of waveforms that meet both the constant amplitude and desired emission constraints. The simplified objective function does not explicitly reduce the energy within the orthogonal complement, though (for a particular waveform initialization) the resulting waveforms after optimization are shown to be near-optimal through comparison to an optimality bound calculated via the Lagrange dual problem [10].

II. Far-Field Emission Model with Signal Constraints

Consider an M element antenna array with an arbitrary geometry satisfying the narrowband assumption (for some transmission bandwidth B) indexed as $m = 0, \ldots, M-1$. It is assumed that this array has full control over the waveforms transmitted by each element (i.e. a digital array). Define $F_m(\theta, \varphi)$ as the time-harmonic (with respect to some center frequency f_c) in-situ far-field antenna pattern for the mth element as a function elevation θ and azimuth φ.[1] It is assumed that the polarization of all antennas are aligned.

Given a set of complex-baseband continuous waveforms $\{s_0(t), s_1(t), \ldots, s_{M-1}(t)\}$ transmitted by the corresponding antenna elements as a function of time t, the complex-baseband far-field emission can be written as

$$g(t, \theta, \varphi) = \sum_{m=0}^{M-1} F_m(\theta, \varphi) s_m(t). \tag{1}$$

[1] In Cartesian coordinates, elevation θ is defined as the angle relative to the xy-plane towards the +z-axis and azimuth φ is defined as the angle relative to the +y-axis towards the +x-axis (i.e. in the xy-plane).

Within this emission structure, define L desired signals $g_\ell(t)$ of pulse duration T to be realized in directions $(\theta_\ell, \varphi_\ell)$ for $\ell = 0, \ldots, L-1$. Using (1), each of these constraints on the emission $g(t, \theta, \varphi)$ can be expressed as

$$g(t, \theta_\ell, \varphi_\ell) = g_\ell(t). \tag{2}$$

To facilitate the design of the M waveforms $s_m(t)$, the constraints in (2) are discretized according to sampling rate f_s. Note that the L desired signals $g_\ell(t)$ must be oversampled with respect to the signal bandwidth B such that sufficient fidelity of the desired signal is maintained. We represent the sampling frequency as $f_\mathrm{s} = \kappa B$, where $\kappa \geq 2$ has been found to be sufficient.

For sampling period $T_\mathrm{s} = 1/f_\mathrm{s}$, define $s_m[n] = s_m(nT_\mathrm{s})$ and $g_\ell[n] = g_\ell(nT_\mathrm{s})$ as the nth sample of the mth waveform and ℓth desired signal, respectively. For pulse duration T, the length of each sequence is $N = f_\mathrm{s}T$. These sequences can be collected into the complex-valued matrices $\mathbf{S} \in \mathbb{C}^{M\times N}$ and $\mathbf{G} \in \mathbb{C}^{L\times N}$ for $[\mathbf{S}]_{m,n} = s_m[n]$ and $[\mathbf{G}]_{\ell,n} = g_\ell[n]$, where $[\bullet]_{i,j}$ represents the (i,j)th element of the matrix. The M complex scalars of the antenna patterns for the L desired transmission directions $(\theta_\ell, \varphi_\ell)$ can also be collected into the matrix $\mathbf{C} \in \mathbb{C}^{M\times L}$ for $[\mathbf{C}]_{m,\ell} = F_m^*(\theta_\ell, \varphi_\ell)$ and $(\bullet)^*$ complex-conjugation. Therefore from (2), the discretized emission constraints can now be written in matrix form as

$$\mathbf{C}^H\mathbf{S} = \mathbf{G}, \tag{3}$$

where $(\bullet)^H$ is the Hermitian transpose.

Given $\mathbf{C}$ and $\mathbf{G}$, the waveform matrix $\mathbf{S}$ is designed such that the constraint of (3) is met. As long as $\mathbf{C}$ has full column rank and $L < M$, there are infinitely many solutions to (3). In Section III, this waveform design is formulated as an optimization problem using two different methods: the minimum-norm method, and the FFRED method, which includes the additional constraint of constant amplitude waveforms.

III. Far-Field Radiated Emission Design

The minimum-norm formulation leads to a closed-form solution satisfying the required signal constraints $\mathbf{C}^H\mathbf{S} = \mathbf{G}$. However, the resulting waveform matrix $\mathbf{S}$ may have an unacceptable peak-to-average power ratio (PAPR), making the set of waveforms undesirable from an implementation standpoint [6], [7]. In the absence of unity PAPR, the waveforms must be scaled so that the maximum amplitude lies within the linear region of the amplifier to ensure that the waveforms are transmitted without distortion. If the waveforms have the same amplitude (unity PAPR), then the amplifiers can be operated in the more power-efficient saturation region. Thus, the PAPR of the waveforms is directly tied to the total energy emitted from the array.

By leveraging the orthogonal complement of $\mathbf{C}$, the PAPR can be reduced while still satisfying the desired signal constraints. Thus, the addition of a constant amplitude constraint to the minimum-norm optimization serves to minimize the energy in the orthogonal complement while achieving both the signal and modulus constraints. To facilitate faster computation, a relaxed problem formulation is developed here. For performance comparison, an optimality bound is also derived via the Lagrange dual function of the original constant amplitude constrained problem.

A. Minimum-norm Solution Method

The minimum-norm optimization problem for determining $\mathbf{S}$ can be written as

$$\begin{aligned} \underset{\mathbf{S}}{\text{minimize}} \quad & \big\|\mathbf{S}\big\|_F^2 \\ \text{subject to} \quad & \mathbf{C}^H\mathbf{S} = \mathbf{G}, \end{aligned} \tag{4}$$

where $\|\mathbf{S}\|_F^2$ is the squared-Frobenius norm defined as

$$\big\|\mathbf{S}\big\|_F^2 = \sum_{m=0}^{M-1}\sum_{n=0}^{N-1} |s_m[n]|^2. \tag{5}$$

The optimization problem in (4) can be reformulated in vectorized notation as

$$\begin{aligned} \underset{\tilde{\mathbf{s}}}{\text{minimize}} \quad & \|\tilde{\mathbf{s}}\|_2^2 \\ \text{subject to} \quad & \mathbf{A}^H\tilde{\mathbf{s}} = \tilde{\mathbf{g}}, \end{aligned} \tag{6}$$

where $\tilde{\mathbf{s}} \in \mathbb{C}^{MN\times 1}$ and $\tilde{\mathbf{g}} \in \mathbb{C}^{LN\times 1}$ are vectorized forms of $\mathbf{S}$ and $\mathbf{G}$, respectively, $\|\tilde{\mathbf{s}}\|_2^2$ is the squared l^2-norm of $\tilde{\mathbf{s}}$, and $\mathbf{A} = \mathbf{I}_N \otimes \mathbf{C}$ for $\mathbf{I}_N$ the $N \times N$ identity matrix, and $\otimes$ the Kronecker product. The entries of the vectorized forms are related to those of the matrices as $[\tilde{\mathbf{s}}]_{m+Mn} = [\mathbf{S}]_{m,n}$ and $[\tilde{\mathbf{g}}]_{\ell+Ln} = [\mathbf{G}]_{\ell,n}$.

Referring to (6) as Problem A, the Lagrangian for this constrained optimization problem is given as

$$\mathcal{L}_A(\tilde{\mathbf{s}}; \lambda) = \tilde{\mathbf{s}}^H\tilde{\mathbf{s}} - \Re\big\{\lambda^H(\mathbf{A}^H\tilde{\mathbf{s}} - \tilde{\mathbf{g}})\big\}, \tag{7}$$

where $\lambda \in \mathbb{C}^{LN\times 1}$ is the Lagrange multiplier pertaining to the emission constraints and $\Re\{\bullet\}$ extracts the real value. The minimum-norm optimization problem is convex with solution [10]

$$\tilde{\mathbf{s}}_{\star,A} = \mathbf{A}\big(\mathbf{A}^H\mathbf{A}\big)^{-1}\tilde{\mathbf{g}}. \tag{8}$$

Equivalently, $\tilde{\mathbf{s}}_{\star,A}$ written in matrix form is

$$\mathbf{S}_{\star,A} = \mathbf{C}\big(\mathbf{C}^H\mathbf{C}\big)^{-1}\mathbf{G}, \tag{9}$$

the rows of which are the M discretized waveforms that are optimal in the minimum-norm sense. However, these waveforms will tend to not be constant amplitude and possess a high PAPR.

B. Utilization of the Orthogonal Complement

By leveraging the orthogonal complement of $\mathbf{C}$, the PAPR of the waveforms can be lowered considerably. Any waveform matrix $\mathbf{S}$ that satisfies the emission constraint $\mathbf{C}^H\mathbf{S} = \mathbf{G}$ has the property

$$\mathbf{S} = \mathbf{S}_{\star,A} + \mathbf{S}_\perp, \tag{10}$$

where $\mathbf{S}_\perp = \mathbf{P}_\perp\mathbf{S}$ is the orthogonal projection of the waveform matrix onto the subspace spanned by the orthogonal complement of $\mathbf{C}$, where

$$\mathbf{P}_\perp = \mathbf{I}_M - \mathbf{C}\big(\mathbf{C}^H\mathbf{C}\big)^{-1}\mathbf{C}^H \tag{11}$$

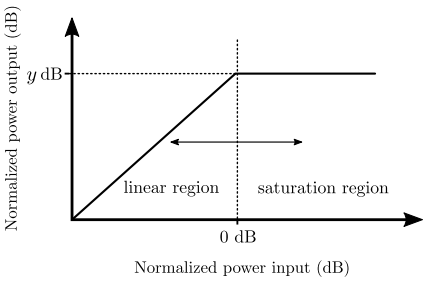

Fig. 1. Gain curve of simplified amplifier model.

is the orthogonal projection matrix. Therefore, the far-field emission of $\mathbf{S}_\perp$ has no impact on the desired emission via $\mathbf{C}^H\mathbf{S}_\perp = \mathbf{0}_{L\times N}$. In the vectorized form, (10) becomes

$$\tilde{\mathbf{s}} = \tilde{\mathbf{s}}_{\star,A} + \tilde{\mathbf{s}}_\perp, \tag{12}$$

where $[\tilde{\mathbf{s}}_\perp]_{m+Mn} = [\mathbf{S}_\perp]_{m,n}$. Thus the property $\mathbf{C}^H\mathbf{S}_\perp = \mathbf{0}_{L\times N}$ is represented as $\mathbf{A}^H\tilde{\mathbf{s}}_\perp = \mathbf{0}_{LN\times 1}$ in vectorized form.

Because $\tilde{\mathbf{s}}_{\star,A}$ and $\tilde{\mathbf{s}}_\perp$ are constructed using orthogonal subspaces, their inner product is $\tilde{\mathbf{s}}_\perp^H\tilde{\mathbf{s}}_{\star,A} = 0$. Therefore, the energy contained in the waveform matrix $\|\tilde{\mathbf{s}}\|_2^2$ is equal to the summation of the energies of the two waveform components,

$$\|\tilde{\mathbf{s}}\|_2^2 = \|\tilde{\mathbf{s}}_{\star,A}\|_2^2 + \|\tilde{\mathbf{s}}_\perp\|_2^2. \tag{13}$$

Thus, any waveform matrix $\mathbf{S}$ (or $\tilde{\mathbf{s}}$) that satisfies $\mathbf{C}^H\mathbf{S} = \mathbf{G}$ (or $\mathbf{A}^H\tilde{\mathbf{s}} = \tilde{\mathbf{g}}$) aside from the minimum-norm solution $\mathbf{S}_{\star,A}$ (or $\tilde{\mathbf{s}}_{\star,A}$) will allocate a portion of its energy to $\mathbf{S}_\perp$ (or $\tilde{\mathbf{s}}_\perp$). The net power efficiency is increased as long as the power efficiency gained through reduction in PAPR exceeds that of any efficiency lost through the addition of energy within the orthogonal complement $\|\tilde{\mathbf{s}}_\perp\|_2^2$. In [6], it was shown that a constant amplitude constrained solution increases the power efficiency of the emission for the case of $L = 2$ beams transmitting a linear frequency modulated radar waveform in one spatial direction and a communications signal in another direction[2].

Figure 1 illustrates the gain curve of a simplified amplifier model used to quantify the power efficiency of a particular waveform matrix. The gain curve is separated into two regions: linear and saturation. The maximum amplifier input in the linear region is normalized to 0 dB. Therefore, to avoid distortion the waveform matrix is normalized by its maximum amplitude, which is denoted as $z = \max_{m,n}\{|s_m[n]|\}$. This normalization corresponds to the well-known procedure of "power back-off".

After normalization, the component of the waveform matrix that contributes to the desired emission is found via the projection $z^{-1}\mathbf{PS}$, where $\mathbf{P} = \mathbf{C}(\mathbf{C}^H\mathbf{C})^{-1}\mathbf{C}^H$ projects onto the subspace spanned by $\mathbf{C}$. For a waveform matrix $\mathbf{S}$ that satisfies $\mathbf{C}^H\mathbf{S} = \mathbf{G}$, this projection is equivalent to $z^{-1}\mathbf{PS} = z^{-1}\mathbf{S}_{\star,A}$. Thus the average power in $z^{-1}\mathbf{S}_{\star,A}$ defines the *Average Directed Power* (ADP) given as

$$\text{ADP} = \frac{\frac{1}{MN}\|\mathbf{S}_{\star,A}\|_F^2}{\max\limits_{m,n}\{|s_m[n]|^2\}}, \tag{14}$$

for $0 \le \text{ADP} \le 1$ with $\text{ADP} = 1$ representing the most power efficient waveform matrix (only obtained when the minimum-norm solution is constant amplitude and $\mathbf{S} = \mathbf{S}_{\star,A}$).

C. Constant-Amplitude Constrained Formulation

The constant amplitude constraint can be incorporated into the optimization problem as $|\tilde{s}_k|^2 - \frac{1}{MN}\|\tilde{\mathbf{s}}\|_2^2 = 0$ for $k = 0, 1, \ldots, MN-1$, where $\tilde{s}_k = [\tilde{\mathbf{s}}]_k$, thus forcing the squared-amplitude to be equal to the average power. By including this constraint the optimization problem becomes

$$\begin{aligned} \underset{\tilde{\mathbf{s}}}{\text{minimize}} \quad & \|\tilde{\mathbf{s}}\|_2^2 \\ \text{subject to} \quad & \mathbf{A}^H\tilde{\mathbf{s}} = \tilde{\mathbf{g}} \\ & |\tilde{s}_k|^2 - \tfrac{1}{MN}\|\tilde{\mathbf{s}}\|_2^2 = 0 \ \forall k. \end{aligned} \tag{15}$$

Modifying the minimum-norm optimization problem from (4) (or (6)) to include any additional constraints introduces a non-zero $\mathbf{S}_\perp$ to the solution (unless the additional constraints are satisfied by the minimum-norm solution). Thus, to satisfy the constant amplitude constraint some amount of energy must be emitted in the directions corresponding to the orthogonal complement of $\mathbf{C}$. However, minimizing $\|\tilde{\mathbf{s}}\|_2^2$ also minimizes the energy contained in the orthogonal complement (i.e. $\|\tilde{\mathbf{s}}_\perp\|_2^2$) according to (13).

The constant amplitude constraint in (15) can be implicitly incorporated by exchanging $\tilde{\mathbf{s}}$ with the waveform model

$$\tilde{\mathbf{s}} = \gamma\exp(j\mathbf{x}), \tag{16}$$

where $j = \sqrt{-1}$, $\gamma \in \mathbb{R}$ is a real-valued amplitude scalar, $\mathbf{x} \in \mathbb{R}^{MN\times 1}$ is a vector of phase values, and the entries of the exponential are defined as $[\exp(j\mathbf{x})]_k = \exp(jx_k)$. Using the waveform model in (16) the optimization problem from (15) can be equivalently represented as

$$\begin{aligned} \underset{\gamma,\mathbf{x}}{\text{minimize}} \quad & \gamma^2 \\ \text{subject to} \quad & \gamma\mathbf{A}^H\exp(j\mathbf{x}) = \tilde{\mathbf{g}}. \end{aligned} \tag{17}$$

The number of optimized parameters for (17) is reduced from $2MN$ real-valued coefficients (MN complex-valued) to $MN+1$ real-valued parameters while removing a constraint from the problem. That said, the optimization problem in (17) is nonconvex and computationally prohibitive to solve directly. However, the Lagrangian of the problem in (17) can be used to find a lower bound for the objective function γ^2 via the Lagrange dual problem [10]. This bound provides a test for solution quality when optimizing parameters $(\gamma, \mathbf{x})$ according to a relaxed version of (17) described in Section III-D.

Referring to (17) as Problem B, the Lagragian for this problem is given as

$$\mathcal{L}_B(\gamma, \mathbf{x}; \lambda) = \gamma^2 - \Re\{\lambda^H(\gamma\mathbf{A}^H\exp(j\mathbf{x}) - \tilde{\mathbf{g}})\}. \tag{18}$$

[2]The communication modulations considered in [6] included rectangular and square-root raised-cosine filtered quadrature phase-shift keying (QPSK) and 4-ary rectangular-filtered continuous phase modulation (CPM) with a modulation index of $1/2$.

The Lagrange dual function (denoted here as $\mathcal{G}(\lambda)$) is found by minimizing [10] $\mathcal{L}_B(\gamma, \mathbf{x}; \lambda)$ over the parameters $(\gamma, \mathbf{x})$ as

$$\mathcal{G}(\lambda) = \inf_{\gamma, \mathbf{x}} \mathcal{L}_B(\gamma, \mathbf{x}; \lambda), \tag{19}$$

which results in the expression

$$\mathcal{G}(\lambda) = -\tfrac{1}{4}\|\mathbf{A}\lambda\|_1^2 + \Re\{\lambda^H \tilde{\mathbf{g}}\}. \tag{20}$$

A derivation for (20) is provided in the appendix. The Lagrange dual function is concave over the Lagrange multipliers (even for nonconvex optimization problems). Thus the Lagrange dual problem is the maximization of the dual function [10].

The optimal function value $\mathcal{G}(\lambda_\star)$ sets a lower bound for the value of the original objective function[3]

$$\mathcal{G}(\lambda_\star) \leq \gamma_\star^2, \tag{21}$$

where $\gamma_\star^2$ is the global minimum of (17). Updating the energy relationship from (13) to incorporate γ (assuming the constraint from (17) holds) yields

$$\gamma^2 = \tfrac{1}{MN}\|\tilde{\mathbf{s}}_{\star,A}\|_2^2 + \tfrac{1}{MN}\|\tilde{\mathbf{s}}_\perp\|_2^2. \tag{22}$$

Therefore, $\mathcal{G}(\lambda_\star)$ is effectively a lower bound on the amount of energy contained in the orthogonal complement (i.e $\|\tilde{\mathbf{s}}_\perp\|_2^2$) that is needed to achieve both the amplitude and emission constraints. Note that the bound in (21) may not be tight. However, a feasible waveform matrix with square-amplitude γ^2 close to this bound gives an indication that the waveform matrix is a near-optimal solution to (17).

D. Relaxed Problem Formulation

To reduce the computational complexity of solving (17) a relaxed problem is formulated that only considers the feasibility of $(\gamma, \mathbf{x})$ as represented by the constraint $\gamma\mathbf{A}^H \exp(j\mathbf{x}) = \tilde{\mathbf{g}}$. This relaxed problem is expressed as

$$\underset{\tilde{\gamma}, \tilde{\mathbf{x}}}{\text{minimize}} \quad \mathcal{J}(\tilde{\gamma}, \tilde{\mathbf{x}}) = \left\|\tilde{\gamma}\mathbf{A}^H \exp(j\tilde{\mathbf{x}}) - \tilde{\mathbf{g}}\right\|_2^2, \tag{23}$$

where $\tilde{\gamma}$ and $\tilde{\mathbf{x}}$ are used to distinguish the parameters from those of (17). The minimum of (23) is guaranteed to be feasible for (17) given that such a point exists, and the quality of the solution found using the relaxed formulation can be determined by comparing $\tilde{\gamma}^2$ to the bound in (21).

A multivariate function can be minimized by first minimizing over a portion of the variables, and then minimizing over the remaining variables. For the objective function $\mathcal{J}(\tilde{\gamma}, \tilde{\mathbf{x}})$, this property is shown via the relationship [10]

$$\inf_{\tilde{\gamma}, \tilde{\mathbf{x}}} \mathcal{J}(\tilde{\gamma}, \tilde{\mathbf{x}}) = \inf_{\tilde{\mathbf{x}}} \left(\inf_{\tilde{\gamma}} \mathcal{J}(\tilde{\gamma}, \tilde{\mathbf{x}}) \right) = \inf_{\tilde{\gamma}} \left(\inf_{\tilde{\mathbf{x}}} \mathcal{J}(\tilde{\gamma}, \tilde{\mathbf{x}}) \right). \tag{24}$$

By minimizing $\mathcal{J}(\tilde{\gamma}, \tilde{\mathbf{x}})$ with respect to $\tilde{\gamma}$, we find that the amplitude has a closed form solution,

$$\tilde{\gamma}(\tilde{\mathbf{x}}) = \frac{\Re\{\tilde{\mathbf{g}}^H \mathbf{A}^H \exp(j\tilde{\mathbf{x}})\}}{\|\mathbf{A}^H \exp(j\tilde{\mathbf{x}})\|_2^2}. \tag{25}$$

[3]The dual function from (20) is found to have *weak duality* except for the case when $N = 1$, which has *strong duality*. Definitions of weak and strong duality can be found in [10].

Thus, the property in (24) can be employed to formulate the problem as a minimization of objective function $\mathcal{J}(\tilde{\gamma}(\tilde{\mathbf{x}}), \tilde{\mathbf{x}})$ over only the phase vector $\tilde{\mathbf{x}}$.

Inserting $\tilde{\gamma}(\tilde{\mathbf{x}})$ from (25) into $\mathcal{J}(\tilde{\gamma}, \tilde{\mathbf{x}})$ from (23) then yields the modified objective function

$$\mathcal{J}(\tilde{\gamma}(\tilde{\mathbf{x}}), \tilde{\mathbf{x}}) = \tilde{\mathcal{J}}(\tilde{\mathbf{x}}) = \|\tilde{\mathbf{g}}\|_2^2 - \frac{\left(\Re\{\tilde{\mathbf{g}}^H \mathbf{A}^H \exp(j\tilde{\mathbf{x}})\}\right)^2}{\|\mathbf{A}^H \exp(j\tilde{\mathbf{x}})\|_2^2}. \tag{26}$$

The gradient of $\tilde{\mathcal{J}}(\tilde{\mathbf{x}})$ with respect to $\tilde{\mathbf{x}}$ can be shown to be

$$\nabla_{\tilde{\mathbf{x}}} \tilde{\mathcal{J}}(\tilde{\mathbf{x}}) = 2\Im\left\{\tilde{\gamma}(\tilde{\mathbf{x}}) \exp(-j\tilde{\mathbf{x}}) \odot \left(\mathbf{A}\left(\tilde{\gamma}(\tilde{\mathbf{x}})\mathbf{A}^H \exp(j\tilde{\mathbf{x}}) - \tilde{\mathbf{g}}\right)\right)\right\}, \tag{27}$$

where $\odot$ is the Hadamard (element-wise) product and $\Im\{\bullet\}$ extracts the imaginary part of the argument. The form of the gradient in (27) can be used in a multitude of different algorithms to converge onto a locally-optimal point of $\tilde{\mathcal{J}}(\tilde{\mathbf{x}})$ [11]. Note that the relaxed objective function in (26) is nonconvex and the obtained solution is dependent on the initialization of $\tilde{\mathbf{x}}$.

For a locally-optimal phase vector $\tilde{\mathbf{x}}_\star$ that minimizes (26) that meets the feasibility requirements of $\tilde{\mathcal{J}}(\tilde{\mathbf{x}}_\star) = 0$, the inequality bound from (21) can be updated as

$$\mathcal{G}(\lambda_\star) \leq \gamma_\star^2 \leq \tilde{\gamma}^2(\tilde{\mathbf{x}}_\star). \tag{28}$$

Using (22), the bound from (28) can be stated in terms of the converged orthogonal energy $\|\tilde{\mathbf{s}}_{\perp,\star}\|_2^2$ as $\frac{1}{MN}\|\tilde{\mathbf{s}}_{\perp,\star}\|_2^2 \geq \mathcal{G}(\lambda\star) - \frac{1}{MN}\|\tilde{\mathbf{s}}_{\star,A}\|_2^2$. Normalizing this lower bound to unity yields the metric

$$\beta = \frac{\frac{1}{MN}\|\tilde{\mathbf{s}}_{\perp,\star}\|_2^2}{\mathcal{G}(\lambda_\star) - \frac{1}{MN}\|\tilde{\mathbf{s}}_{\star,A}\|_2^2} \geq 1, \tag{29}$$

where β represents the ratio of the converged average orthogonal power $\frac{1}{MN}\|\tilde{\mathbf{s}}_{\perp,\star}\|_2^2$ to $(\mathcal{G}(\lambda_\star) - \frac{1}{MN}\|\tilde{\mathbf{s}}_{\star,A}\|_2^2)$ which is the theoretical lower bound on average orthogonal power. Likewise, using (14) the bound from (28) can be rearranged in terms of the ADP of the converged solution as

$$\frac{\text{ADP}}{\text{ADP}_{\text{opt}}} \leq 1, \tag{30}$$

where $\text{ADP} = \frac{1}{MN}\|\mathbf{S}_{\star,A}\|_F^2 \tilde{\gamma}^{-2}(\tilde{\mathbf{x}}_\star)$ is the average directed power of the obtained solution and $\text{ADP}_{\text{opt}} = \frac{1}{MN}\|\mathbf{S}_{\star,A}\|_F^2 \mathcal{G}^{-1}(\lambda_\star)$ is the theoretical upper bound on average directed power for a constant amplitude solution.

IV. Analysis of the Relaxed Problem Formulation

A Monte Carlo analysis is used to characterize the performance of the relaxed FFRED formulation from Section III-D for the cases of $L \in \{2, 3, 4\}$ simultaneous signals. In each case the desired transmission angles $(\theta_\ell, \varphi_\ell)$ and signals $g_\ell(t)$ are based on randomized parameters, and the converged values of $\tilde{\gamma}^2(\tilde{\mathbf{x}}_\star)$ are compared to $\mathcal{G}(\lambda_\star)$ using the metrics defined in (29) and (30).

The desired signals are chosen to have a constant amplitude, which is known to decrease the amount of energy in the

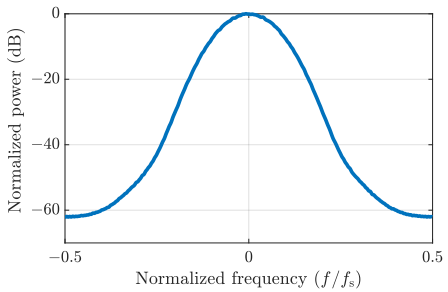

Fig. 2. Power Spectral Density of random PCFM waveform with Gaussian shaping filter of duration $3T_p$ sampling frequency $f_s = 3/T_p$.

orthogonal complement needed to achieve a feasible solution [6]. Thus, the desired signals conform to

$$g_\ell(t) = \begin{cases} a_\ell \exp\left(j\psi_\ell(t)\right) & 0 \le t \le T \\ 0 & \text{otherwise} \end{cases}, \tag{31}$$

where a_ℓ is a real-valued, positive scalar and $\psi_\ell(t)$ is the continuous phase function. It is assumed that $g_0(t)$ is the dominant signal in energy relative to the other signals (e.g. a radar transmission). Therefore, $a_0 = 1$ while the remaining $L-1$ signal amplitudes are randomly drawn according to $10\log_{10}|a_\ell|^2 \sim U[-20,-10]$, where $U[a,b]$ is the uniform probability distribution over the interval $[a,b]$. Thus the remaining amplitudes range from -20 dB to -10 dB relative to the dominant signal.

The continuous phase function $\psi_\ell(t)$ is randomly generated using a random parameterization of the polyphase-coded frequency-modulated (PCFM) framework given by [12]

$$\psi_\ell(t) = \int_0^t \sum_{n=0}^{N_p-1} \alpha_{\ell,n} h(\zeta - nT_p) d\zeta, \tag{32}$$

where $\alpha_{\ell,n} \sim U[-\pi,\pi]$ are the N_p PCFM code values, $h(t)$ is a shaping filter, and $T_p = T/N_p \approx 1/B$. Here, $h(t)$ is chosen to be a truncated-Gaussian window with duration $3T_p$ and unit area. The sampling rate is $f_s = 3B = 3/T_p$ and $N_p = 40$ random code values per pulse equates to $N = 120$ samples in each discretized waveform. The power spectral density of this random pulsed waveform is shown in Figure 2. This signal could represent either a radar or communications transmission (e.g. FM noise radar [13], continuous phase modulation (CPM) communications [14]).

For this analysis, consider an $M = 16$ element uniform linear array (ULA) with half-wavelength spacing aligned in the $\theta = 0^\circ$ plane with array boresight toward $\varphi = 0^\circ$. The antenna patterns from (2) are assumed to be omnidirectional in the $\theta = 0^\circ$ plane and normalized to unity, thus the mth in-situ antenna pattern is expressed as

$$F_m(\theta = 0^\circ, \varphi) = \exp\left(jm\frac{2\pi}{\lambda} d \sin\varphi\right). \tag{33}$$

The desired transmission directions in the elevation dimension are fixed to $\theta_\ell = 0^\circ \ \forall \ell$; thus, the signals are separated in azimuth φ_ℓ. The dominant signal is directed towards array boresight at $\varphi_0 = 0^\circ$ while the remaining signal directions are sequentially determined according to independent draws

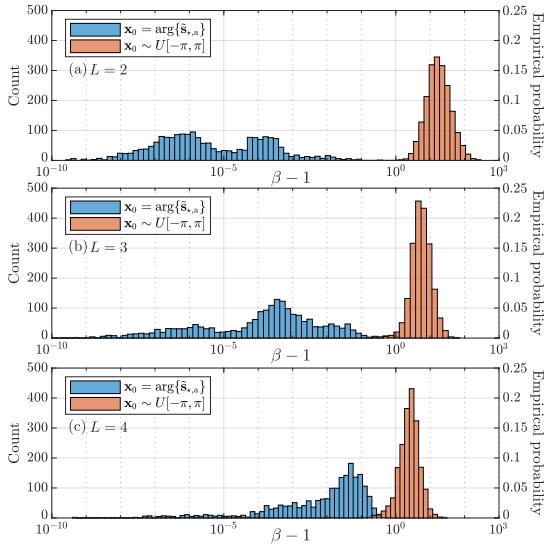

Fig. 3. Histogram of $\beta - 1$ from (29) for (a) $L = 2$, (b) $L = 3$, and (c) $L = 4$ desired transmit signals over 2000 Monte Carlo trials with minimum-norm (blue) and random (red) phase initializations for $\tilde{\mathbf{x}}$.

from $\sin\varphi_\ell \sim U[-1,1]$. If a randomly chosen transmission angle falls within the array peak-to-null beamwidth of a previously chosen angle (i.e. $|\sin\varphi_\ell - \sin\varphi_i| < 2/M$ for $i = 0,\ldots,\ell-1$) a new angle is randomly selected until the condition is satisfied.

A total of 2000 Monte Carlo trials were performed for two different phase initializations (i.e. $\tilde{\mathbf{x}}_0$) for each of the $L \in \{2,3,4\}$ desired signals: uniformly distributed initialization, $\tilde{\mathbf{x}}_0 \sim U[-\pi,\pi]$; and initialized using the phase of the minimum-norm solution, $\tilde{\mathbf{x}}_0 = \arg\{\tilde{\mathbf{s}}_{\star,A}\}$, where $\arg\{\bullet\}$ extracts the phase. The limited-memory Broyden-Fletcher-Goldfarb-Shanno (L-BFGS) algorithm [11] (coupled with a backtracking line search) was used to minimize the relaxed problem from (23) for each Monte Carlo trial. A total of 10 prior gradients are kept during the optimization process for estimation of the local second-order properties of $\tilde{\mathcal{J}}(\tilde{\mathbf{x}})$. The algorithm is terminated when $\tilde{\mathcal{J}}(\tilde{\mathbf{x}}) < \|\tilde{\mathbf{g}}\|_2^2 \times 10^{-12}$. The dual function $\mathcal{G}(\lambda)$ from (20) is maximized using the CVX Matlab toolbox [15].

Figure 3 shows the histograms of $\beta - 1 \ge 0$ from (29) for the minimum-norm phase initializations (blue) and the random phase initializations (red) for (a) $L = 2$, (b) $L = 3$, and (c) $L = 4$ desired signals. It is observed that the bound from (21) is tight for the minimum-norm phase initialization since $\beta - 1$ takes on values on the order of 10^{-10}. Recall that β represents the ratio of the obtained average orthogonal power to its theoretical lower bound. Therefore, the energy in the orthogonal complement is marginally greater than the theoretical lower bound for all three cases, increasing slightly when L is increased. The random phase initialization falls into a local minimum of $\tilde{J}(\tilde{\mathbf{x}})$, resulting in a significant increase in β and thereby indicating that the energy in the orthogonal complement is not near the theoretical bound for this initialization.

Figure 4 depicts the histograms of $1 - \frac{\text{ADP}}{\text{ADP}_{\text{opt}}} \ge 0$ from (30) for the minimum-norm phase initialization and $L = 2,3,4$

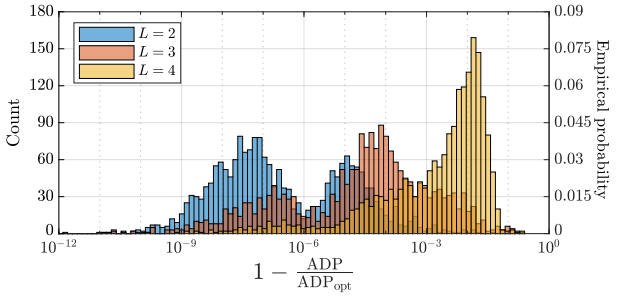

Fig. 4. Histogram of $1 - \frac{\text{ADP}}{\text{ADP}_{\text{opt}}}$ for $L = 2$ (blue), $L = 3$ (red), and $L = 4$ (yellow) desired transmit signals over 2000 Monte Carlo trial for the minimum-norm phase initialization, $\tilde{\mathbf{x}}_0 = \arg\{\tilde{\mathbf{s}}_{\star,A}\}$.

desired signals. These results indicate that the solutions found using the relaxed problem from (23) with the minimum-norm phase initialization are *near-optimal* in terms of power efficiency relative to the original problem in (17).

V. Conclusions

The ability to emit multiple signals simultaneously from a digital array provides the flexibility to efficiently use all available resources (i.e. time, frequency, space, and power) for multiple functions (e.g. radar and/or communications). The FFRED formulation considers efficient use of all the resources while conforming to practical waveform constraints (e.g. constant amplitude). The Lagrange dual problem of FFRED provides an optimality bound upon the amount of energy in the orthogonal complement needed to achieve a solution. It is shown that a near-optimal (in terms of orthogonal complement energy) set of waveform can be designed via minimization of a relaxed FFRED formulation initialized with the phase of the minimum-norm solution.

Appendix

The Lagrange dual function $\mathcal{G}(\lambda)$ for Lagrangian $\mathcal{L}_B(\gamma, \mathbf{x}; \lambda)$ can be written as a successive minimization over variables γ and $\mathbf{x}$ as [10]

$$\mathcal{G}(\lambda) = \inf_{\mathbf{x}} \left(\inf_{\gamma} \mathcal{L}_B(\gamma, \mathbf{x}; \lambda) \right). \tag{34}$$

The problem $\inf_\gamma \mathcal{L}_B(\gamma, \mathbf{x}; \lambda)$ can be solved by taking the derivative of $\mathcal{L}_B(\gamma, \mathbf{x}; \lambda)$ from (18) with respect to γ and setting equal to zero as

$$\tfrac{\partial}{\partial \gamma} \mathcal{L}_B(\gamma, \mathbf{x}; \lambda) = 0 = 2\gamma - \Re\big\{\lambda^H \mathbf{A}^H \exp(j\mathbf{x})\big\}. \tag{35}$$

Thus, the closed-form expression for γ as a function of $\mathbf{x}$ and λ is

$$\gamma(\mathbf{x}; \lambda) = \tfrac{1}{2} \Re\big\{\lambda^H \mathbf{A}^H \exp(j\mathbf{x})\big\}. \tag{36}$$

Inserting (36) into the original Lagrangian from (18) then yields the updated form

$$\tilde{\mathcal{L}}(\mathbf{x}; \lambda) = -\tfrac{1}{4} \Big(\Re\big\{\lambda^H \mathbf{A}^H \exp(j\mathbf{x})\big\} \Big)^2 + \Re\{\lambda^H \tilde{\mathbf{g}}\}. \tag{37}$$

The dual function is now found by minimizing $\tilde{\mathcal{L}}(\mathbf{x}; \lambda)$ with respect to $\mathbf{x}$ via the gradient

$$\nabla_{\mathbf{x}} \tilde{\mathcal{L}}(\mathbf{x}; \lambda) = 0 = -\tfrac{1}{2} \Re\big\{\lambda^H \mathbf{A}^H \exp(j\mathbf{x})\big\} \Im\big\{\exp(-j\mathbf{x}) \odot (\mathbf{A}\lambda)\big\}. \tag{38}$$

Solutions to (38) occur when $\mathbf{x}$ has the form

$$\mathbf{x} = \arg\big\{\mathbf{A}\lambda\big\} + \pi \mathbf{u}, \tag{39}$$

where $\arg\{\bullet\}$ extracts the phase and $\mathbf{u} \in \mathbb{Z}^{MN \times 1}$ for $\mathbb{Z}$ the set containing all integers.

Observing (37), the Lagrangian is minimized with respect to $\mathbf{x}$ when $(\Re\{\lambda^H \mathbf{A}^H \exp(j\mathbf{x})\})^2$ is maximized. Inserting the form of $\mathbf{x}$ from (39) into this expression yields

$$\Re\big\{\lambda^H \mathbf{A}^H \exp(j\mathbf{x})\big\} = \sum_k b_k |\mathbf{a}_k^H \lambda|, \tag{40}$$

where $b_k \in \{-1, +1\}$. Therefore, to maximize $(\Re\{\lambda^H \mathbf{A}^H \exp(j\mathbf{x})\})^2$ the sign variable b_k needs to be $b_k = -1 \ \forall k$ (all odd entries in $\mathbf{u}$) or $b_k = 1 \ \forall k$ (all even entries in $\mathbf{u}$). Either selection results in the expression

$$(\Re\{\lambda^H \mathbf{A}^H \exp(j\mathbf{x}_\star)\})^2 = \|\mathbf{A}\lambda\|_1^2, \tag{41}$$

where $\mathbf{x}_\star$ corresponds to $\mathbf{x}$ from (39) when the entries of $\mathbf{u}$ are either all odd or all even. Inserting the expression from (41) into (37) yields the form of the dual function $\mathcal{G}(\lambda)$ from (20).

References

[1] D.J. Rabideau and P.A. Parker, "Ubiquitous MIMO multifunction digital array radar... and the role of time-energy management in radar," MIT Lincoln Lab, Tech. Rep., 2004.

[2] G.C. Tavik, C.L. Hilterbrick, J.B. Evins, J.J. Alter, J.G. Crnkovich, J.W. de Graaf, W. Habicht, G.P. Hrin, S.A. Lessin, D.C. Wu, and S.M. Hagewood, "The advanced multifunction RF concept," *IEEE Trans. Microw. Theory Tech.*, vol. 53, no. 3, pp. 1009–1020, Mar. 2005.

[3] J.S. Herd and M.D. Conway, "The evolution to modern phased array architectures," *Proc. IEEE*, vol. 104, no. 3, pp. 519–529, Mar. 2016.

[4] S.H. Talisa, K.W. O'Haver, T.M. Comberiate, M.D. Sharp, and O.F. Somerlock, "Benefits of digital phased array radars," *Proc. IEEE*, vol. 104, no. 3, pp. 530–543, Mar. 2016.

[5] C. Fulton, M. Yeary, D. Thompson, J. Lake, and A. Mitchell, "Digital phased arrays: challenges and opportunities," *Proc. IEEE*, vol. 104, no. 3, pp. 487–503, Mar. 2016.

[6] C. Sahin, P.M. McCormick, and B. Ravenscroft, "Embedding communications into radar emissions by transmit waveform diversity," in *Radar & Communication Spectrum Sharing*, S.D. Blunt and E.S. Perrins, eds. IET, 2018.

[7] P.M. McCormick, S.D. Blunt, and J.G. Metcalf, "Simultaneous radar and communications emission from a common aperture, part I: theory," *IEEE Radar Conf.*, May 2017.

[8] P.M. McCormick, A.J. Duly, B. Ravenscroft, J.G. Metcalf, and S.D. Blunt, "Simultaneous radar and communications emission from a common aperture, part II: experimentation," *IEEE Radar Conf.*, May 2017.

[9] H.H. Bauschke, P.L. Combettes, and D.R. Luke, "Phase retrieval, error reduction algorithm, and Fienup variants: a view from convex optimization," *JOSA A*, vol. 19, no. 7, pp. 1334–1345, 2002.

[10] S. Boyd and L. Vandenberghe, *Convex Optimization*. Cambridge University Press, 2004.

[11] J. Nocedal and S. Wright, *Numerical Optimization*. Springer Science & Business Media, 2006.

[12] S.D. Blunt, M. Cook, J. Jakabosky, J. de Graaf, and E. Perrins, "Polyphase-coded FM (PCFM) radar waveforms, part I: implementation," *IEEE Trans. Aerosp. Electron. Syst.*, vol. 50, no. 3, pp. 2218–2229, Jul. 2014.

[13] J. Jakabosky, S.D. Blunt, and B. Himed, "Spectral-shape optimized FM noise radar for pulse agility," *IEEE Radar Conf.*, May 2016.

[14] J.G. Proakis, "Digital communications," *McGraw-Hill, New York, 5th ed.*, 2008.

[15] M. Grant and S. Boyd, "CVX: Matlab software for disciplined convex programming, version 2.1," http://cvxr.com/cvx, Mar. 2014.